Electronic Supplementary Material (ESI) for Journal of Materials Chemistry A.

Supporting Information

One Arrow, Two Eagles: Li-Argyrodite Solid-State Electrolytes with Lithium Compatibility and Air Stability for All-Solid-State Batteries

Daoxi Wang[a], Haiting Shi[a], Wenhui Cui[a], Hao Li[b], Jiarong Niu[a], Shuo Wang[a], Zhiwei Xu*[a]

[a] State Key Laboratory of Separation Membranes and Membrane Processes, School of Textile Science and Engineering, Tiangong University, Tianjin 300387, China
[b] Key Laboratory of Neutron Physics, Institute of Nuclear Physics and Chemistry, China Academy of Engineering Physics, Mianyang 621999, China

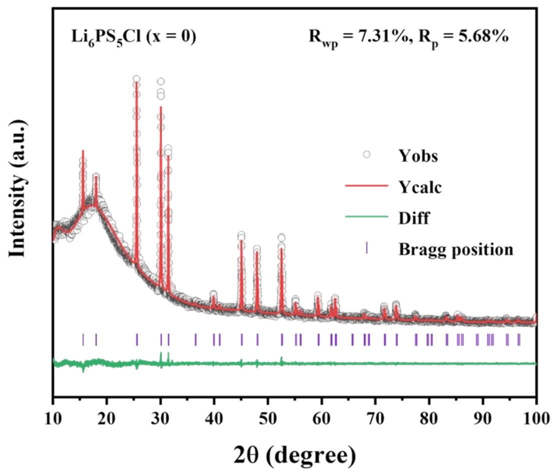

Fig. S1 XRD Rietveld refinement results of Li_6PS_5Cl electrolyte powder at room temperature.

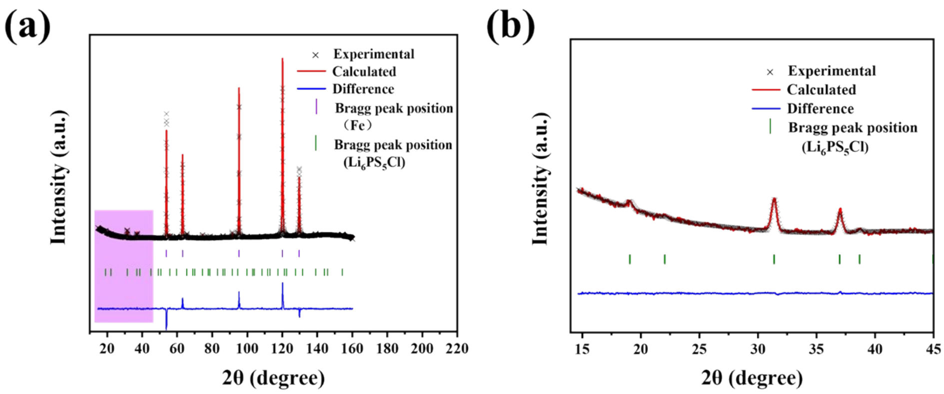

Fig. S2 (a) Rietveld refined ND pattern for the Li_6PS_5Cl; (b) Rietveld refined ND（Li_6PS_5Cl）

* Corresponding author. E-mail address: xuzhiwei@tiangong.edu.cn(Zhiwei Xu)

magnification from 15° to 45°.

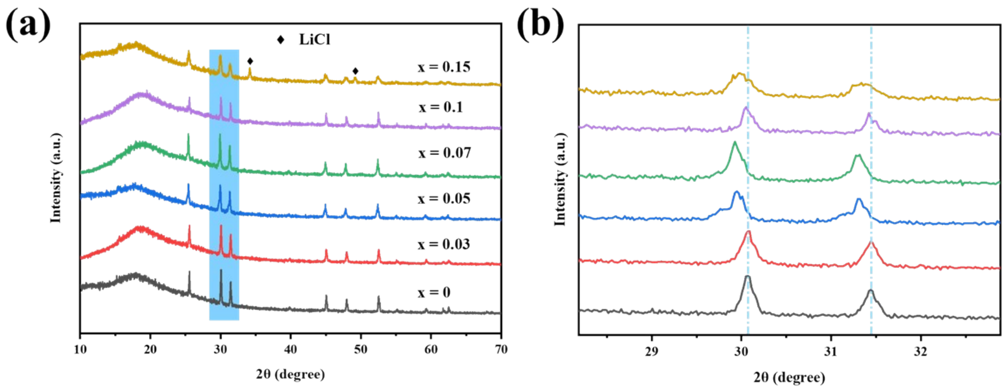

Fig. S3 Zr-substituted Li sites: (a) XRD patterns of $Li_{6-4x}Zr_xPS_{5-2x}O_{2x}Cl$ ($0 \le x \le 0.15$) at 10° to 70° and (b) magnified XRD patterns at 27.5° to 33.5°.

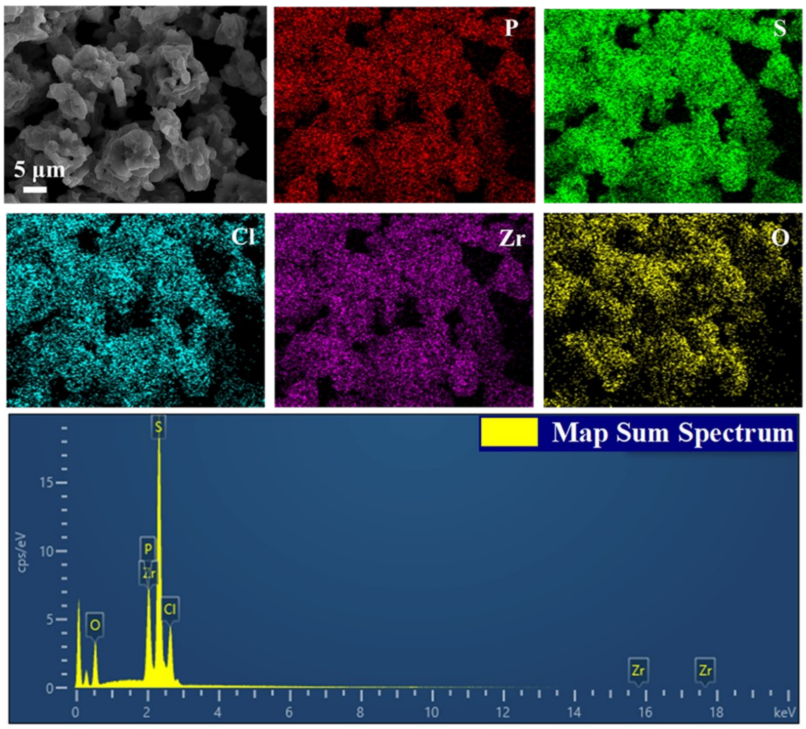

Fig. S4 SEM and EDS mapping of $Li_{6+x}P_{1-x}Zr_xS_{5-2x}O_{2x}Cl$ (x = 0.01) electrolyte.

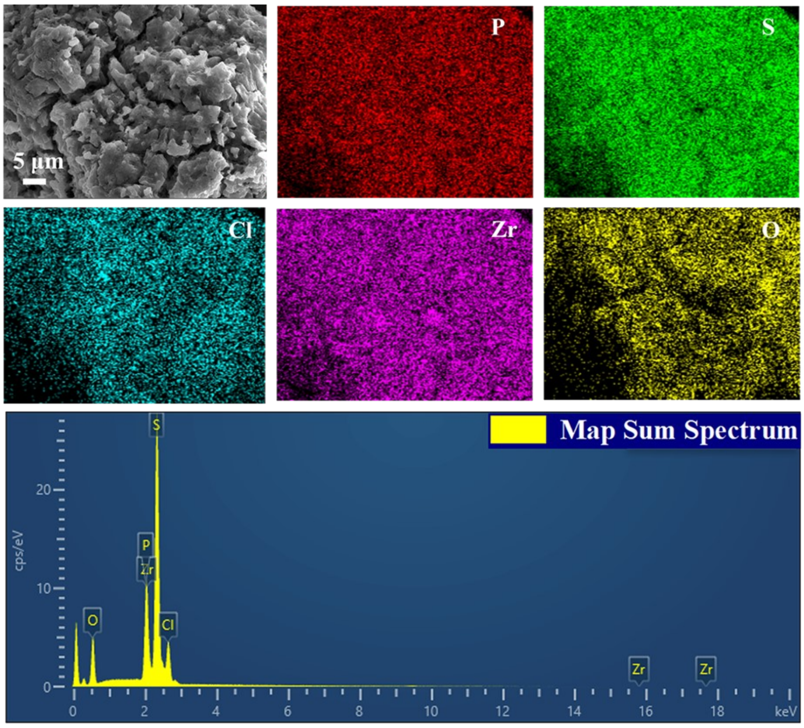

Fig. S5 SEM and EDS mapping of $Li_{6+x}P_{1-x}Zr_xS_{5-2x}O_{2x}Cl$ (x = 0.03) electrolyte.

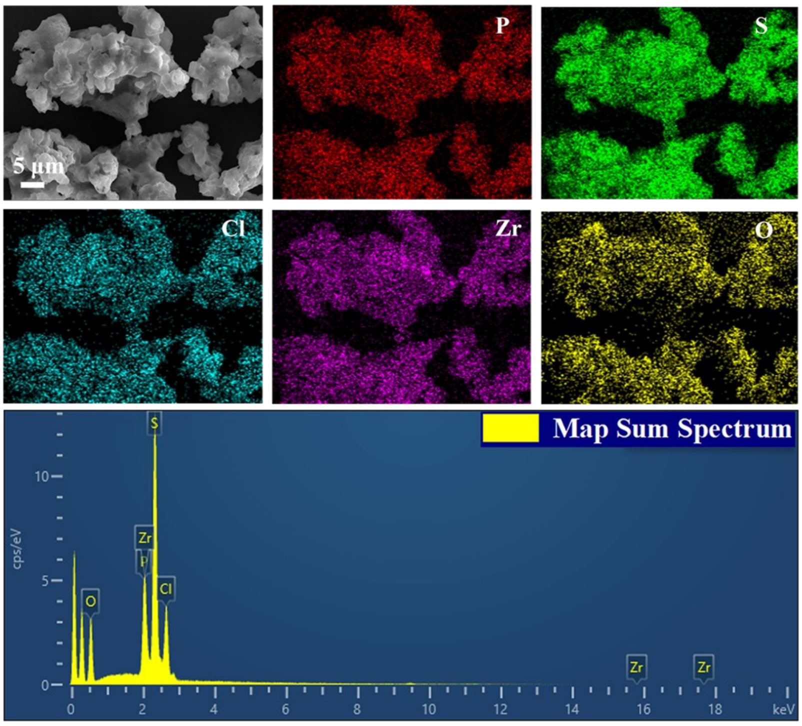

Fig. S6 SEM and EDS mapping of $Li_{6+x}P_{1-x}Zr_xS_{5-2x}O_{2x}Cl$ (x = 0.07) electrolyte.

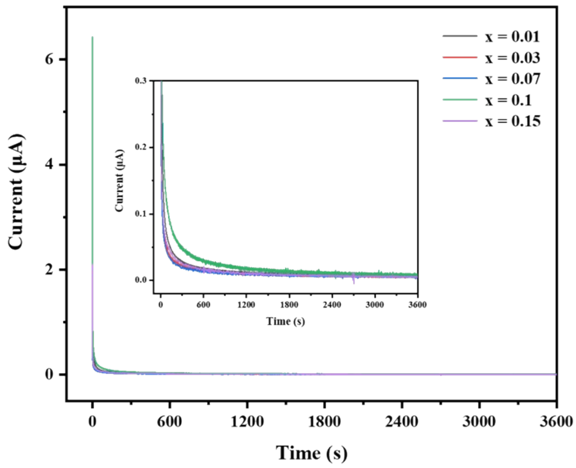

Fig. S7 DC polarization curves for $Li_{6+x}P_{1-x}Zr_xS_{5-2x}O_{2x}Cl$ (x = 0.01, 0.03, 0.07, 0.1, 0.15) electrolytes.

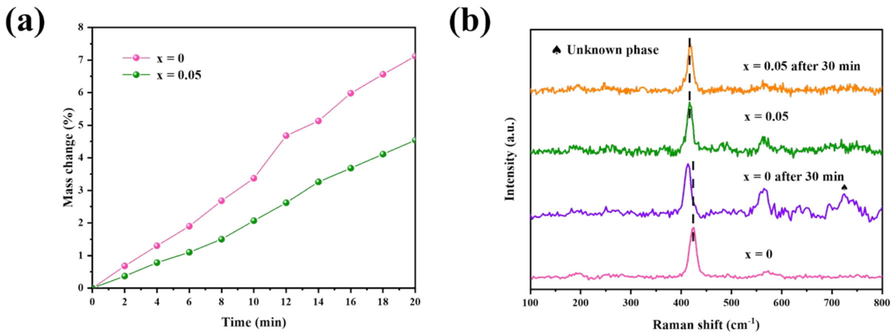

Fig. S8 (a) Mass changes for SSEs as a function of time after exposure to humid air; (b) Raman spectra of the Li_6PS_5Cl and $Li_{6.05}P_{0.95}Zr_{0.05}S_{4.9}O_{0.1}Cl$ electrolytes before and after exposure to humid air.

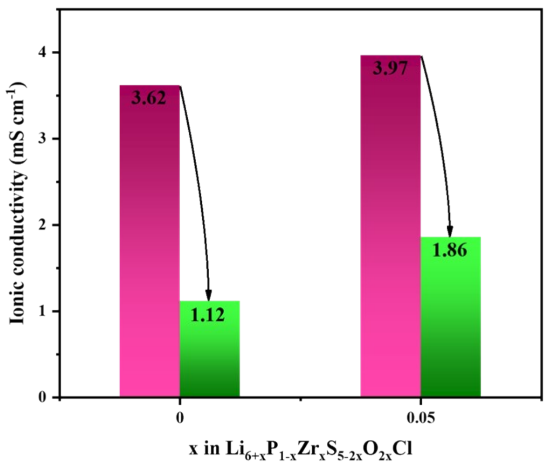

Fig. S9 Changes in ionic conductivity of $Li_{6+x}P_{1-x}Zr_xS_{5-2x}O_{2x}Cl$ (x = 0, 0.05) electrolytes before and after exposure to air.

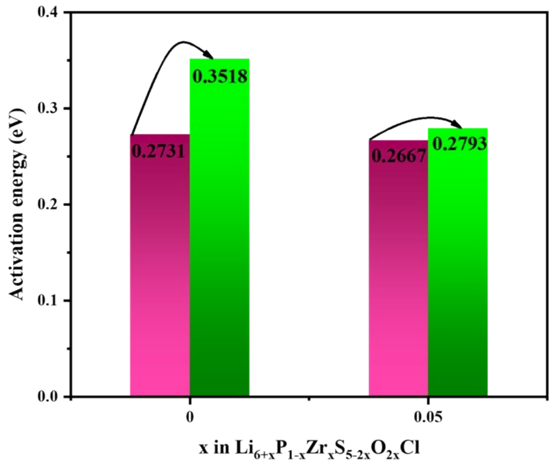

Fig. S10 Changes in activation energy of $Li_{6+x}P_{1-x}Zr_xS_{5-2x}O_{2x}Cl$ (x = 0, 0.05) electrolytes before and after exposure to air.

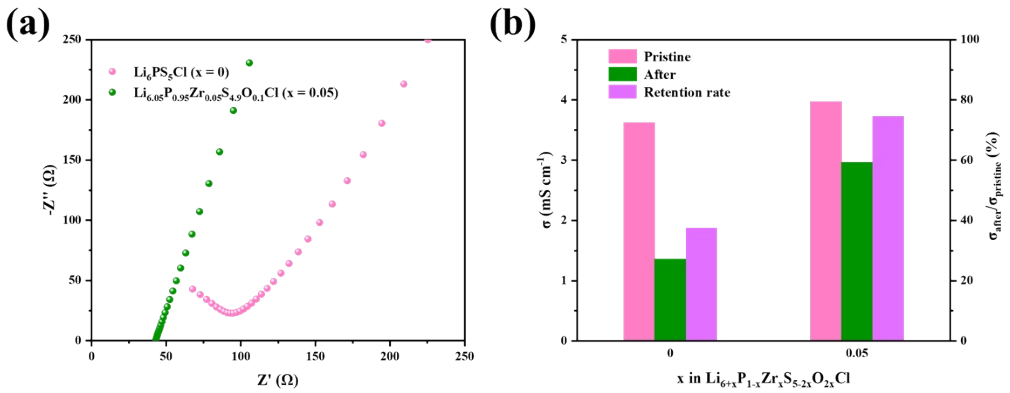

Fig. S11 (a) EIS of Li_6PS_5Cl and $Li_{6.05}P_{0.95}Zr_{0.05}S_{4.9}O_{0.1}Cl$ electrolytes after post-annealing; (b) Ionic conductivity and restoration ratio of Li_6PS_5Cl and $Li_{6.05}P_{0.95}Zr_{0.05}S_{4.9}O_{0.1}Cl$ electrolytes after post annealing.

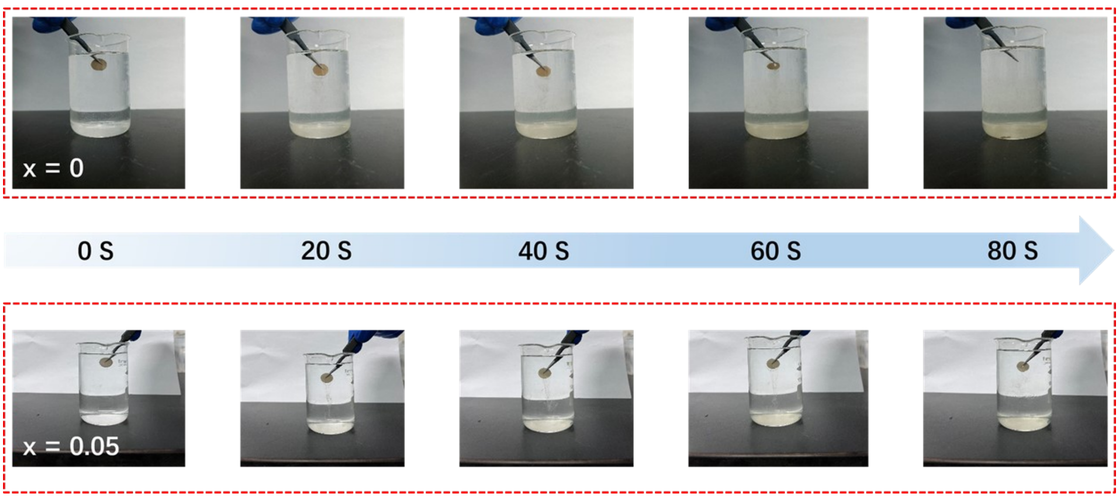

Fig. S12 Optical photographs of Li_6PS_5Cl (x = 0) and $Li_{6.05}P_{0.95}Zr_{0.05}S_{4.9}O_{0.1}Cl$ (x = 0.05) electrolytes completely immersed in deionized water at room temperature.

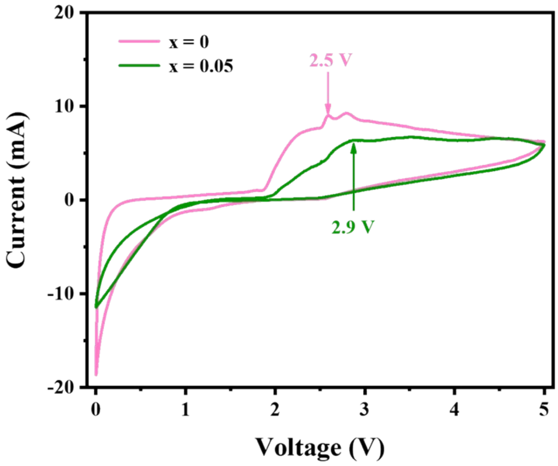

Fig. S13 CV test of assembled C@Cu/$Li_{6+x}P_{1-x}Zr_xS_{5-2x}O_{2x}Cl$/Li asymmetric cell (x = 0, 0.05).

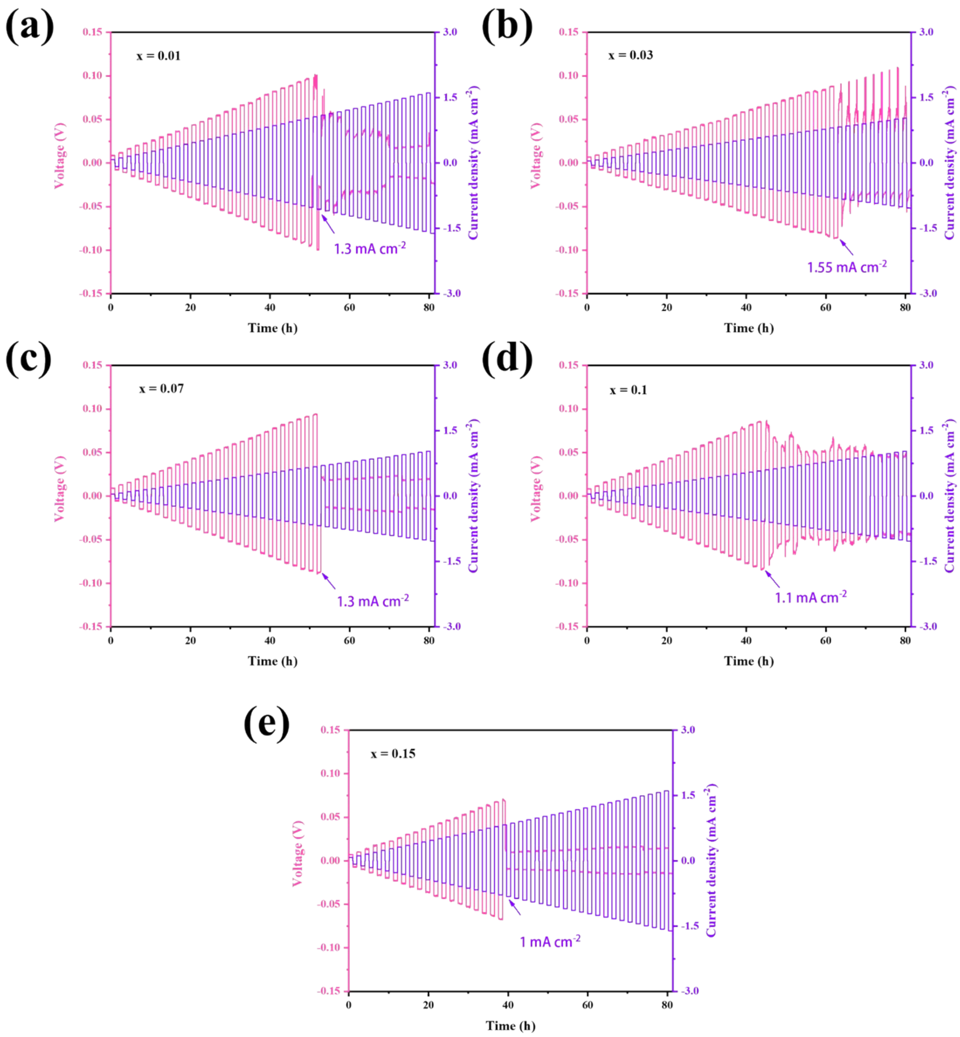

Fig. S14 Li symmetric cells with different ZrO_2 co-substitution levels were subjected to constant current cycling at 298 K at progressively increasing current densities, where (a) x = 0.01, (b) x =

0.03, (c) x = 0.07, (d) x = 0.1, and (e) x = 0.15.

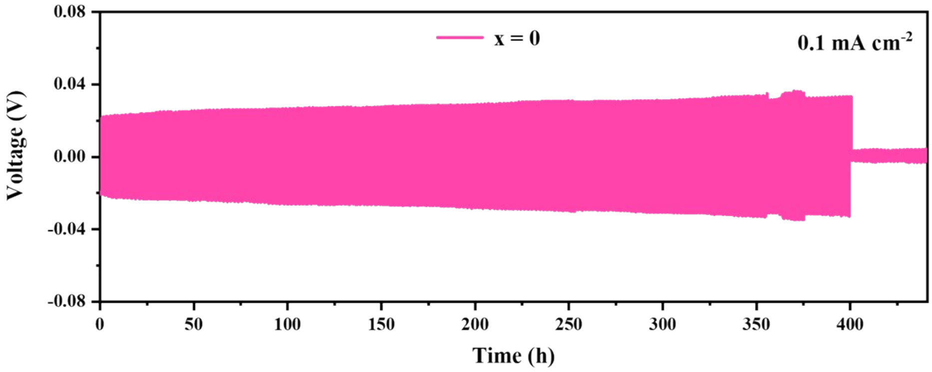

Fig. S15 Galvanostatic cycling of Li/Li_6PS_5Cl/Li symmetric cell at the current density of 0.1 mA cm^{-2} for 0.1 mAh cm^{-2}.

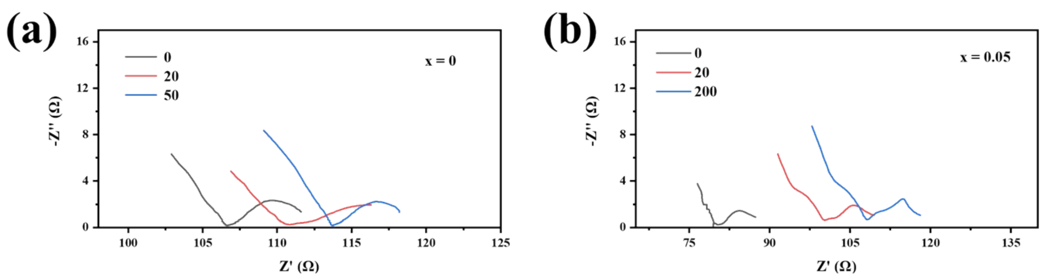

Fig. S16 The impedance spectral changes of (a) Li/Li_6PS_5Cl/Li and (b) Li/$Li_{6.05}P_{0.95}Zr_{0.05}S_{4.9}O_{0.1}Cl$/Li symmetric cells after different lithium stripping/plating durations.

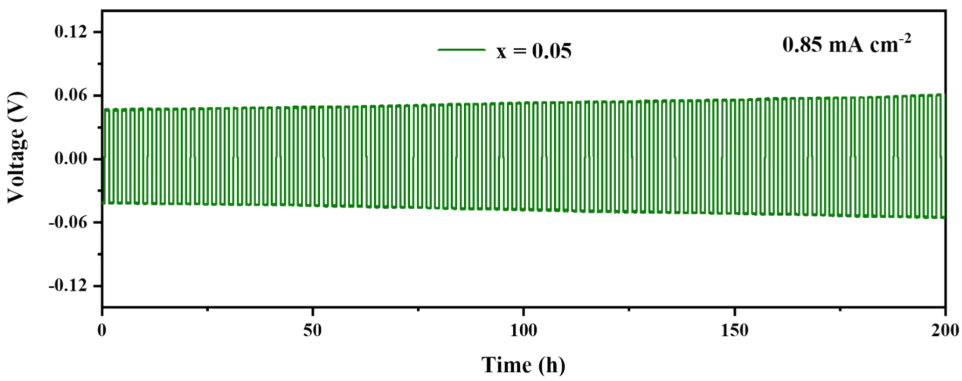

Fig. S17 Galvanostatic cycling of the Li symmetric cells with $Li_{6.05}P_{0.95}Zr_{0.05}S_{4.9}O_{0.1}Cl$ electrolyte at 0.85 mA cm^{-2}/0.85 mAh cm^{-2}.

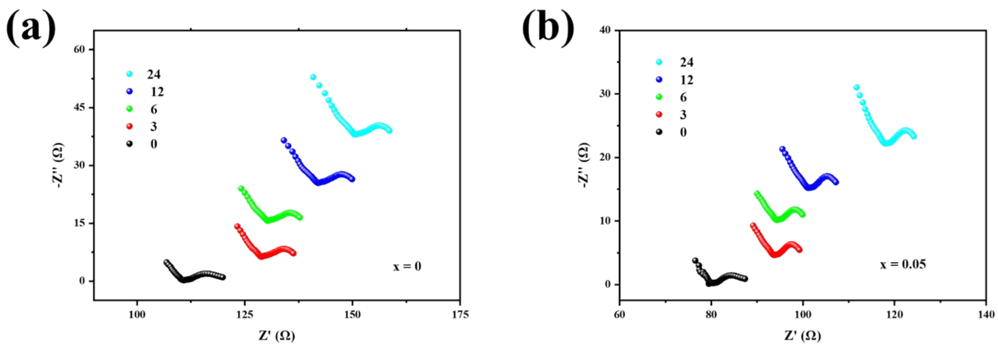

Fig. S18 Time-dependent EIS spectra of Li symmetric cells with different sulfide electrolytes: (a) pristine Li_6PS_5Cl (x = 0) and (b) $Li_{6.05}P_{0.95}Zr_{0.05}S_{4.9}O_{0.1}Cl$ (x = 0.05) electrolytes.

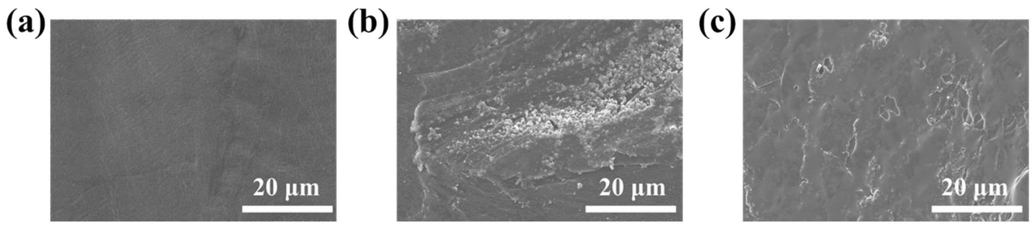

Fig. S19 (a) SEM images of pristine Li metal surface. SEM images of Li surface after cycling with (b) Li_6PS_5Cl electrolyte and (c) pristine $Li_{6.05}P_{0.95}Zr_{0.05}S_{4.9}O_{0.1}Cl$ electrolyte, respectively.

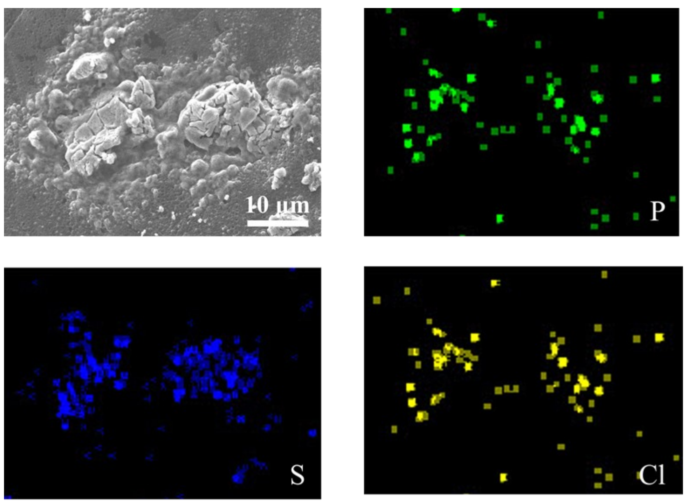

Fig. S20 The corresponding EDS mapping of Li surface after cycling with pristine Li_6PS_5Cl electrolyte.

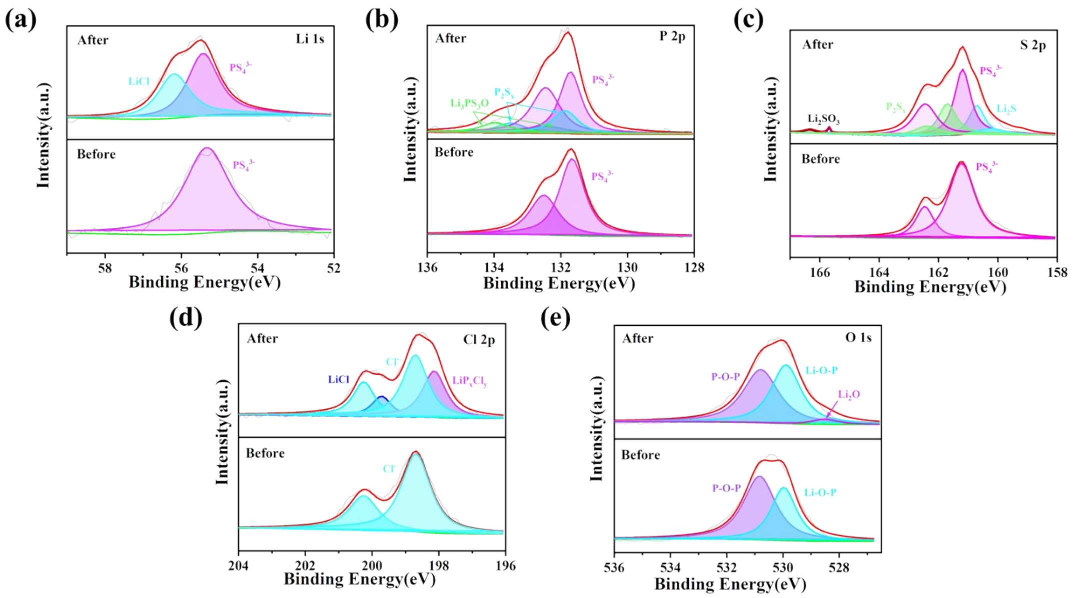

Fig. S21 (a) XPS deconvolution spectra of Li 1s, (b) P 2p, (c) S 2p, (d) Cl 2p and (e) O 1s region of fresh and after cycling Li/$Li_{6.05}P_{0.95}Zr_{0.05}S_{4.9}O_{0.1}Cl$ interface.

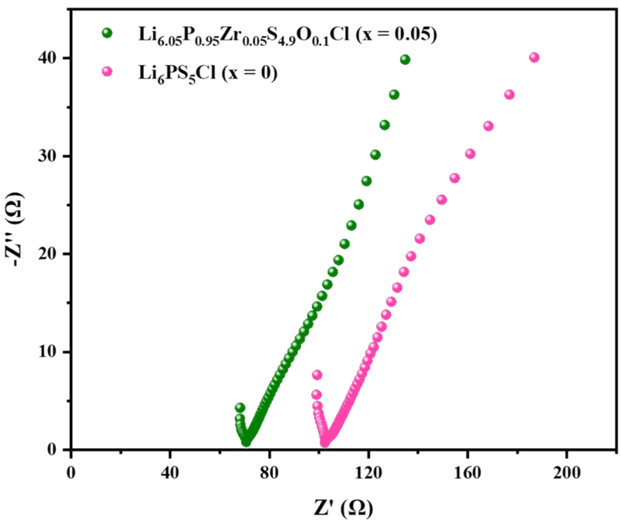

Fig. S22 Nyquist plots of $LiCoO_2$/ $Li_{6.05}P_{0.95}Zr_{0.05}S_{4.9}O_{0.1}Cl$/Li and $LiCoO_2$/Li_6PS_5Cl/Li batteries.

Table S1 Crystallographic data of Li_6PS_5Cl obtained from Rietveld refinement.

Li_6PS_5Cl structure from X-ray power diffraction data (space group F-43m);
$\lambda_1(Cu\text{-}K_{\alpha1})$ = 1.5406 Å; $\lambda_2(Cu\text{-}K_{\alpha2})$ = 1.5444 Å
a = 9.848228 Å;
R_{wp} = 7.31%; R_p = 5.68%; χ^2 = 1.604

Atom	Wyckoff site	x	y	z	Occ.	U_{iso}[$Å^2$]
Li1	48h	0.3203	0.0182	0.6798	0.5000	0.0478
P1	4b	0.0000	0.0000	0.5000	1.0000	0.0197

S1	16e	0.1200	-0.1200	0.6200	1.0000	0.0328
S2	4d	0.2500	0.2500	0.7500	0.3850	0.0354
S3	4a	0.0000	0.0000	1.0000	0.6150	0.0208
Cl1	4d	0.2500	0.2500	0.7500	0.6150	0.0354
Cl2	4a	0.0000	0.0000	1.0000	0.3850	0.0208

Table S2 Crystallographic data of $Li_{6.05}P_{0.95}Zr_{0.05}S_{4.9}O_{0.1}Cl$ obtained from Rietveld refinement.

$Li_{6.05}P_{0.95}Zr_{0.05}S_{4.9}O_{0.1}Cl$ structure from X-ray power diffraction data (space group F-43m); λ_1(Cu-K$_{\alpha1}$) = 1.5406 Å; λ_2(Cu-K$_{\alpha2}$) = 1.5444 Å a = 9.851008 Å; R_{wp} = 8.25%; R_p = 5.68%; χ^2 = 1.216						
Atom	**Wyckoff site**	**x**	**y**	**z**	**Occ.**	**U_{iso}[Å^2]**
Li1	48h	0.3201	0.0199	0.6799	0.5150	0.0137
P1	4b	0.0000	0.0000	0.5000	0.9090	0.0244
Zr1	4b	0.0000	0.0000	0.5000	0.0910	0.0244
S1	16e	0.1200	-0.1200	0.6200	0.9836	0.0416
O1	16e	0.1200	-0.1200	0.6200	0.0164	0.0416
S2	4d	0.2500	0.2500	0.7500	0.3850	0.0263
S3	4a	0.0000	0.0000	1.0000	0.6150	0.0221
Cl1	4d	0.2500	0.2500	0.7500	0.6150	0.0263
Cl2	4a	0.0000	0.0000	1.0000	0.3850	0.0221

Table S3 Crystallographic data (atomic coordinates, occupancy, and Beq) of Li_6PS_5Cl, obtained from Rietveld refinement of neutron diffraction data.

Li_6PS_5Cl structure from neutron diffraction data (space group F-43m); λ_1 = 1.8838 Å; a = 9.851711 Å; Fit residuals (R_{wp}, R_{exp}, R_p): 4.786%, 5.211%, 3.718%;						
Atom	**Wyckoff site**	**x**	**y**	**z**	**Occ.**	**Beq**

Li1	48h	0.3203	0.0182	0.6798	0.50000	2.99951
P1	4b	0.0000	0.0000	0.5000	1.00000	0.00000
S1	16e	0.1200	-0.1200	0.6200	1.00000	0.97127
S2	4d	0.2500	0.2500	0.7500	0.21789	0.01653
S3	4a	0.0000	0.0000	1.0000	0.58577	0.07156
Cl1	4d	0.2500	0.2500	0.7500	0.78211	0.00283
Cl2	4a	0.0000	0.0000	1.0000	0.41423	0.04195

Table S4 Crystallographic data (atomic coordinates, occupancy, and Beq) of $Li_{6.05}P_{0.95}Zr_{0.05}S_{4.9}O_{0.1}Cl$, obtained from Rietveld refinement of neutron diffraction data.

$Li_{6.05}P_{0.95}Zr_{0.05}S_{4.9}O_{0.1}Cl$ structure from neutron diffraction data (space group F-43m); λ_1 = 1.8838 Å; a = 9.854896 Å; Fit residuals (R_{wp}, R_{exp}, R_p): 8.727%, 4.166%, 5.801%;						
Atom	**Wyckoff site**	**x**	**y**	**z**	**Occ.**	**Beq**
Li1	48h	0.3203	0.0182	0.6798	0.50000	3.00000
P1	4b	0.0000	0.0000	0.5000	0.18997	2.36554
S1	16e	0.1200	-0.1200	0.6200	0.86720	3.00000
S2	4d	0.2500	0.2500	0.7500	0.04249	2.18362
S3	4a	0.0000	0.0000	1.0000	0.54228	0.00000
Cl1	4d	0.2500	0.2500	0.7500	0.95751	2.18362
Cl2	4a	0.0000	0.0000	1.0000	0.45772	0.00000
Zr1	4b	0.0000	0.0000	0.5000	0.86720	2.36554
O1	16e	0.1200	-0.1200	0.6200	0.13280	3.00000

Table S5 Summary of the sulfide electrolyte-based Li-Li symmetric cell performance.

Electrolyte	CCD (mA cm^{-2})	Cycling Current Density (mA cm^{-2})	Cut-off Capacity (mAh cm^{-2})	Cycling Time (h)	Operating temperature	Reference
		0.1	**0.1**	**800**	**RT**	
$Li_{6.05}P_{0.95}Zr_{0.05}S_{4.9}O_{0.1}Cl$	**1.7**	**0.5**	**0.5**	**400**	**RT**	**This work**
		0.85	**0.85**	**200**	**RT**	
$Li_6PS_{4.7}O_{0.3}Br$	0.89	0.1	-	560	RT	1
$Li_{5.5}PS_{4.425}O_{0.075}Cl_{1.5}$	-	0.4	0.2	150	RT	2
$Li_{6.2}P_{0.8}Sn_{0.2}S_5I$	1.26	0.1	0.1	700	RT	3
$Li_{6.03}P_{0.97}Se_{0.03}S_5Cl$	0.6	0.1	-	185	RT	4
$Li_6P_{0.925}Sb_{0.075}S_5Cl$	1.2	0.1	0.1	800	RT	5
		0.2	0.2	1200	RT	
$Li_{5.6}Cu_{0.2}PS_{4.8}Br_{1.2}$	1.2	0.5	1	240	RT	6
		1	3	120	50℃	
		0.1	0.1	600	RT	
$Li_{6.04}P_{0.98}Bi_{0.02}S_{4.97}O_{0.03}Cl$	1.1					7
		1	1	200	RT	
$Li_{5.6}PS_{4.6}Cl_{1.0}Br_{0.4}$	0.35	0.2	-	500	RT	8
$Li_{5.5}P_{0.9}Sn_{0.1}S_{4.2}O_{0.2}Cl_{1.6}$	1.2	0.5	0.5	200	RT	9
$Li_{5.7}Zn_{0.15}PS_{4.85}O_{0.15}Br$	0.78	0.78	0.39	140	RT	10
		0.2	-	300	RT	
LPSScO(0.15)-22.5LiS	0.6					11
		0.3	-	200	RT	
$Li_7P_{2.88}Nb_{0.12}S_{10.7}O_{0.3}$	1.16	0.2	0.2	300	RT	12
$Li_{6.3}P_{0.7}Sn_{0.3}S_{4.4}O_{0.6}I$	0.75	0.2	0.1	180	RT	13
LiFSI@LPS	0.7	0.3	0.6	360	RT	14
$Li_7P_2S_8I$	0.2	0.2	0.2	83	RT	15

Table S6 Comparison of physicochemical properties of $Li_{6.05}P_{0.95}Zr_{0.05}S_{4.9}O_{0.1}Cl$ electrolyte with other representative sulfide electrolytes.

Sulfide solid electrolyte	Ionic conductivity (RT, mS cm^{-1})	Electronic conductivity (RT, S cm^{-1})	Air stability	Interface with Li metal	Reference
$Li_{6.05}P_{0.95}Zr_{0.05}S_{4.9}O_{0.1}Cl$	**3.97**	**6.11×10^{-10}**	**Good**	**Good**	**This work**
Li_6PS_5Br	2.76	1.45×10^{-8}	Bad	Bad	16
Li_6PS_5Cl	1.46	8.98×10^{-9}	Bad	Bad	17
Li_3PS_4	0.389	1.2×10^{-9}	Bad	Bad	18
$Li_7P_3S_{11}$	0.81	2.92×10^{-8}	Bad	Bad	12
$Li_{10}GeP_2S_{12}$	12	9×10^{-9}	Bad	Bad	19
Li_2SnS_3	0.015	-	Good	Bad	20
Li_4SnS_4	0.07	-	Good	Bad	21
$Li_6PS_5Cl_{0.3}F_{0.7}$	0.71	9.85×10^{-10}	-	Good	22
$Li_{6.3}P_{0.9}Mg_{0.1}S_5Cl_{0.8}F_{0.2}$	1.7	1.03×10^{-9}	-	Good	23

References

1. Z. X. Zhang, L. Zhang, X. L. Yan, H. Q. Wang, Y. Y. Liu, C. Yu, X. T. Cao, L. van Eijck and B. Wen, *J. Power Sources*, 2019, **410**, 162-170.
2. L. F. Peng, S. Q. Chen, C. Yu, C. C. Wei, C. Liao, Z. K. Wu, H. L. Wang, S. J. Cheng and J. Xie, *ACS Appl. Mater. Interfaces*, 2022, **14**, 4179-4185.
3. F. P. Zhao, J. W. Liang, C. Yu, Q. Sun, X. N. Li, K. Adair, C. H. Wang, Y. Zhao, S. M. Zhang, W. H. Li, S. X. Deng, R. Y. Li, Y. N. Huang, H. Huang, L. Zhang, S. Q. Zhao, S. G. Lu and X. L. Sun, *Adv. Energy Mater.*, 2020, **10**.
4. H. M. Kim, Y. Subramanian and K. S. Ryu, *Electrochim. Acta*, 2023, **442**.
5. H. Liu, Q. S. Zhu, Y. H. Liang, C. Wang, D. B. Li, X. X. Zhao, L. Gao and L. Z. Fan, *Chem. Eng. J.*, 2023, **462**.
6. Z. Jiang, Y. Liu, H. L. Peng, J. R. Li, X. Xu, H. Su, Y. Zhong, X. L. Wang, C. D. Gu and J. P. Tu,

Energy Stor. Mater., 2023, **56**, 300-309.

7. H. Liu, Q. S. Zhu, C. Wang, G. X. Wang, Y. H. Liang, D. B. Li, L. Gao and L. Z. Fan, *Adv. Funct. Mater.*, 2022, **32**.
8. Y. Subramanian, R. Rajagopal and K. S. Ryu, *J. Power Sources*, 2022, **520**.
9. G. Y. Li, S. P. Wu, H. P. Zheng, Y. Yang, J. Y. Cai, H. Zhu, X. Huang, H. Z. Liu and H. N. Duan, *Adv. Funct. Mater.*, 2023, **33**.
10. T. Chen, L. Zhang, Z. X. Zhang, P. Li, H. Q. Wang, C. Yu, X. L. Yan, L. M. Wang and B. Xu, *ACS Appl. Mater. Interfaces*, 2019, **11**, 40808-40816.
11. Y. Subramanian, R. Rajagopal, S. Kang, Y. J. Jung and K. S. Ryu, *J Energy Storage*, 2023, **68**.
12. Z. Jiang, T. B. Liang, Y. Liu, S. Z. Zhang, Z. X. Li, D. H. Wang, X. L. Wang, X. H. Xia, C. D. Gu and J. P. Tu, *ACS Appl. Mater. Interfaces*, 2020, **12**, 54662-54670.
13. T. Chen, D. W. Zeng, L. Zhang, M. Yang, D. W. Song, X. L. Yan and C. Yu, *J. Energy Chem.*, 2021, **59**, 530-537.
14. X. L. Fan, X. Ji, F. D. Han, J. Yue, J. Chen, L. Chen, T. Deng, J. J. Jiang and C. S. Wang, *Sci. Adv.*, 2018, **4**.
15. E. Rangasamy, Z. C. Liu, M. Gobet, K. Pilar, G. Sahu, W. Zhou, H. Wu, S. Greenbaum and C. D. Liang, *J. Am. Chem. Soc.*, 2015, **137**, 1384-1387.
16. Z. Jiang, C. Yu, S. Chen, C. Wei, C. Liao, Z. Wu, S. Chen, S. Cheng and J. Xie, *Scr. Mater.*, 2023, **227**, 115303.
17. B. W. Taklu, Y. Nikodimos, H. K. Bezabh, K. Lakshmanan, T. M. Hagos, T. A. Nigatu, S. K. Merso, H. Y. Sung, S. C. Yang, W. N. Su and B. J. Hwang, *Nano Energy*, 2023, **112**.
18. Y. Ni, C. Huang, H. Liu, Y. H. Liang and L. Z. Fan, *Adv. Funct. Mater.*, 2022, **32**.
19. N. Kamaya, K. Homma, Y. Yamakawa, M. Hirayama, R. Kanno, M. Yonemura, T. Kamiyama, Y. Kato, S. Hama, K. Kawamoto and A. Mitsui, *Nat. Mater.*, 2011, **10**, 682-686.
20. J. A. Brant, D. M. Massi, N. A. W. Holzwarth, J. H. MacNeil, A. P. Douvalis, T. Bakas, S. W. Martin, M. D. Gross and J. A. Aitken, *Chem. Mater.*, 2015, **27**, 189-196.
21. T. Kaib, S. Haddadpour, M. Kapitein, P. Bron, C. Schröder, H. Eckert, B. Roling and S. Dehnen, *Chem. Mater.*, 2012, **24**, 2211-2219.
22. F. P. Zhao, Q. Sun, C. Yu, S. M. Zhang, K. Adair, S. Z. Wang, Y. L. Liu, Y. Zhao, J. W. Liang, C. H. Wang, X. N. Li, X. Li, W. Xia, R. Y. Li, H. Huang, L. Zhang, S. Q. Zhao, S. G. Lu and

X. L. Sun, *ACS Energy Lett.*, 2020, **5**, 1035-1043.

23. C. Liu, B. T. Chen, T. R. Zhang, J. C. Zhang, R. Y. Wang, J. Zheng, Q. J. Mao and X. F. Liu, *Angew. Chem. Int. Ed.*, 2023, DOI: 10.1002/anie.202302655.